Comparative Analysis of Microsatellite Instability-High BRAF V600E–Mutated Versus MSI-H BRAF-Wild-Type Colorectal Cancers, Including Tumor Microenvironment, Associated Genomic Alterations, and Immuno-Metabolomic Biomarkers

Abstract 3066

Mohamed E. Salem[1], Thierry Andre[2], Sherif El-Refai[3], Christopher Thompson[3], Elizabeth Mauer[3], Thomas J George[4], Josep Tabernero[5], Frank Sinicrope[6], Jeanne Tie[7], Scott Kopetz[8], Eric Van Cutsem[9], Sara Lonardi[10], Michael J Overman[2], and David Foureau[1]

[1]Levine Cancer Institute, Charlotte, NC, USA, [2]Assistance Publique Hospitaux de Paris, Paris, France, [3]Tempus Labs Inc, Chicago, IL, USA, [4]University of Florida, Gainesville, FL, USA, [5]Vall d'Hebron University Hospital, Barcelona, Spain, [6]Mayo Clinic, Rochester, MN, [7]Walter+Eliza Hall Institute of Medical Research, Parkville, Australia, [8]MD Anderson, Houston, TX, USA, [9]University of Leuven, Belgium, [10]Instituto Oncologico Veneto, Italy

INTRODUCTION

Colorectal Cancer (CRC)

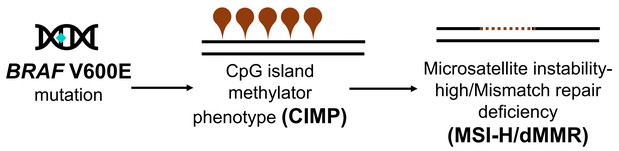

The impact of coexisting BRAF V600E mutations on the tumor microenvironment (TME) and immunometabolic features of MSI-H/dMMR CRC is not well characterized.

We evaluated the relationship between *BRAF* mutations, TME, and immunometabolic features in a patient cohort with MSI-H/dMMR CRC.

METHODS

De-identified records of patients (N=459) with CRC sequenced by the Tempus xT next-generation sequencing (NGS) assay were retrospectively analyzed

Loci analyzed, IHC

MSI-H was determined by assessment of 239 loci and dMMR by IHC

DNA seq, RNA seq, IHC data

Tumor mutational burden (TMB), neoantigen tumor burden (NTB, NeoScan), PD-L1 expression, immune infiltration, and canonical immuno-metabolomic pathways assessed

Overview of Cohort Demographics

Characteristic	Overall, N=459	*BRAF*^{WT}, n=336	*BRAF V600E*^{mut}, n=123
***Gender, n (%)**			
Female	269 (59%)	185 (55%)	84 (69%)
Unknown	1	0	1
***Age, Median (IQR)**	69 (57, 78)	62 (51, 73)	76 (70, 85)
Unknown	126	108	18
Race, n (%)			
White	227 (83%)	170 (82%)	57 (86%)
Black/African American	20 (7.3%)	16 (7.7%)	4 (6.1%)
Asian	3 (1.1%)	3 (1.4%)	0 (0%)
Other	24 (8.8%)	19 (9.1%)	5 (7.6%)
Unknown	185	128	57
Stage, n (%)			
Stage I	19 (5.0%)	17 (6.0%)	2 (2.0%)
Stage II	81 (21%)	60 (21%)	21 (21%)
Stage III	90 (24%)	63 (22%)	27 (27%)
Stage IV	190 (50%)	141 (50%)	49 (49%)
Unknown	79	55	24

**Indicates significance by BRAF V600E status following Pearson's Chi-squared test, Fisher's exact test, or Wilcoxon rank-sum test; Age reflects data at diagnosis; Stage reflects data available closest to biopsy collection. ‡ Percentages reflect number of patients for each metric out of all patients with reported data for that respective metric (total less missing population).*

Table 1. Description of the patient cohort analyzed.

SUMMARY

- In a cohort of 459 MSI-H/dMMR CRCs, ***BRAF* V600E^{mut} CRCs exhibited hyperproliferative characteristics associated with broad metabolic reprogramming**.
- *BRAF* V600E^{mut} and *BRAF*^{wt} MSI-H/dMMR CRCs exhibited **similar NTB and T cell infiltration**, suggesting both are equally likely to benefit from immune checkpoint inhibitors.

RESULTS

Overview of Molecular Characteristics

Characteristic	Overall, N=459	*BRAF*^{WT}, n=336	*BRAF V600E*^{mut}, n=123	p-value
MSI-H, n (%)	444 (98%)	321 (97%)	123 (100%)	0.041*
Unknown	4	4	0	
TMB-H, n (%)	428 (96%)	305 (95%)	123 (100%)	0.008*
Unknown	15	15	0	
NTB, Median (IQR)	15 (10, 20)	15 (10, 20)	15 (12, 20)	0.4
Unknown	38	35	3	
†**PDL-1+, n (%)**	37 (26%)	27 (23%)	10 (36%)	0.2
Unknown	316	221	95	

**Indicates significance by BRAF V600E status following Pearson's Chi-squared test, Fisher's exact test, or Wilcoxon rank-sum test.*
†PD-L1 Status was only available for patients whose samples were assessed in-house by immunohistochemical staining.
‡ Percentages reflect number of patients for each metric out of all patients with reported data for that respective metric (total less missing population).

Table 2. BRAF V600E^{mut} patient tumors were slightly more likely to be MSI-H and TMB-H (in fact, 100% in the current cohort for both) than BRAF V600E^{WT} patient tumors. In a reduced cohort of patient tumors that underwent internal IHC, BRAF V600E^{mut} tumors demonstrated a trend towards more PD-L1 positivity, albeit non-significant in the reduced cohort.

Genomic Differences Between *BRAF* V600E^{mut} and *BRAF*^{WT} MSI-H/dMMR CRCs

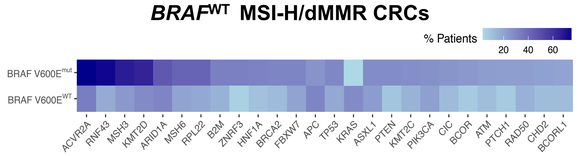

**Comparisons were made by Pearson's Chi-squared tests with false-discovery rate correction for multiple comparisons. Percentages reflect the proportion of patients in each group with a Pathogenic or Likely-Pathogenic somatic short variant.*

Figure 1. When compared to *BRAF*^{WT} tumors, *BRAF* V600E^{mut} tumors harbored, among other differences, a greater frequency of *MSH6* (42% vs. 20%), *B2M* (33% vs. 16%), *BRCA2* (31% vs. 12%), *ATM* (23% vs. 12%), and *TP53* (30% vs. 19%) but a lower frequency of *MSH2* (3.3% vs. 11%), all q<0.05.

Acknowledgements: We thank Amrita A. Iyer, PhD and Matthew Kase for poster assembly and review.

Correspondence: Mohamed.Salem@atriumhealth.org

***BRAF* V600E^{mut} Impacts Tumor CRCs Immune Microenvironment**

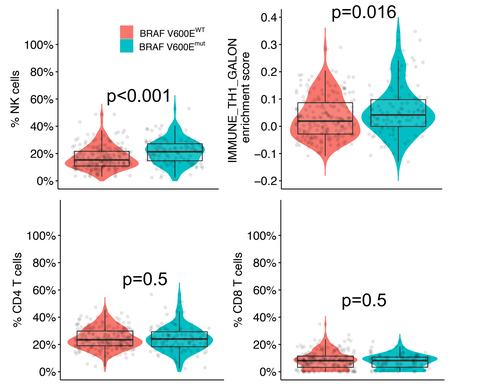

Infiltrating immunocytes were compared by Wilcoxon rank-sum tests. IMMUNE_TH1_GALON enrichment compared through differential expression (see Figure 5**). *N_{Total} patient tumors with RNA-Seq. data available= 324.*

Figure 2. Proportions of infiltrating immune cells were estimated through RNA-seq*. The proportion of natural killer (NK) cells was significantly higher in BRAF V600Emut compared with BRAFWT (median 21% vs. 15%, p <0.001) while no significant differences were found amongst CD4+ and CD8+ T cells. IMMUNE_TH1_GALON showed significant up-regulation in BRAF V600Emut tumors (**see Figure 5**).

***BRAF* V600E^{mut} CRCs Show Accelerated Growth and Metabolic Reprograming**

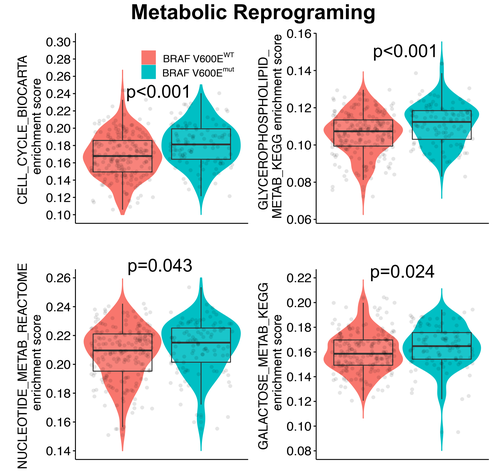

**N_{Total} patient tumors with RNA-Seq. data available= 324.*

Figure 4. Five pathways demonstrated significant upregulation (**see Figure 5**) among BRAF V600Emut tumors, 4 of which included: cyclin-dependent cell signaling, glycerophospholipid metabolism, galactose metabolism and nucleotide metabolism.

Cancer Stem Cell Pathways Are Downregulated in *BRAF* V600E^{mut} Tumors

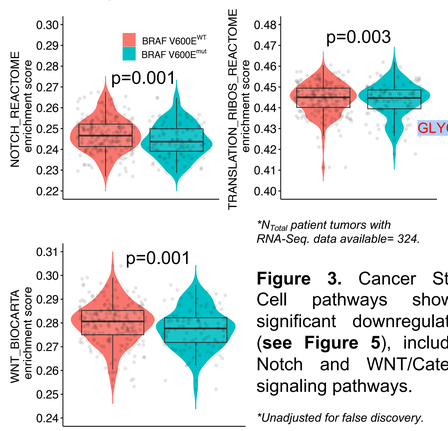

**N_{Total} patient tumors with RNA-Seq. data available= 324.*

Figure 3. Cancer Stem Cell pathways showed significant downregulation (**see Figure 5**), including Notch and WNT/Catenin signaling pathways.

**Unadjusted for false discovery.*

Immune-related Pathways Differentially Expressed by *BRAF* V600E Status

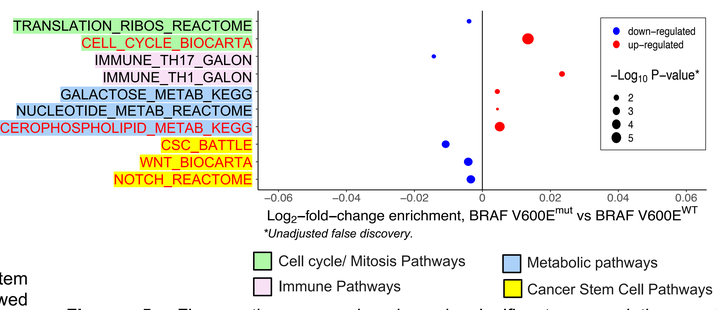

Figure 5. Five pathways each showed significant upregulation and downregulation among BRAF V600E^{mut} tumors (p<0.05). Enrichment of pathways highlighted in red were significantly different following false discovery adjustment. Pathway enrichment scores computed through GSVA (full form) were compared between BRAF V600E^{mut} and BRAF V600E^{WT} via differential expression analysis. Differentially expressed pathways (at 5% alpha level) are shown. Pathways differentially expressed after false discovery adjustment are represented in red.

Peter Mac — Peter MacCallum Cancer Centre, Victoria Australia
Walter+Eliza Hall Institute of Medical Research — DISCOVERIES FOR HUMANITY
Vall d'Hebron Hospital
KU LEUVEN
UFHealth CANCER CENTER
TEMPUS
Atrium Health Levine Cancer Institute